2022 44th Annual International Conference of
the IEEE Engineering in Medicine & Biology Society (EMBC)
Scottish Event Campus, Glasgow, UK, July 11-15, 2022

High Classification Accuracy of Touch Locations from S1 LFPs Using CNNs and Fastai*

Bret A. See and Joseph T. Francis, *Member, IEEE*

Abstract— **The primary somatosensory cortex (S1) is a region often targeted for input via somatosensory neuroprosthesis as tactile and proprioception are represented in S1. How this information is represented is an ongoing area of research. Neural signals are high-dimensional, making accurate models for decoding a significant challenge. Artificial neural networks (ANNs) have proven efficient at classification tasks in multiple fields. Moreover, ANNs allow for transfer learning, which exploits feature extraction trained on a large and more general dataset than may be available for a particular problem. In this work, convolutional neural networks (CNN), used for image recognition, were fine-tuned with somatosensory cortical recordings during experiments with naturalistic touch stimuli. We created a highly accurate (> 96% correct) classifier for cutaneous stimulation locations as part of a somatosensory neuroprosthesis pipeline. Here we present the classifier results.**

Clinical Relevance— **Our work provides a method for classifying cortical activity in brain-machine interface applications, specifically towards somatosensory neuroprosthetics.**

I. Introduction

Local Field Potential (LFP) recordings in the cortex are an important form of electrophysiological information used for many Brain-Machine Interface (BMI) applications. Previously, LFPs have been used for decoding the onset and intensity of pain[1], intended motor actions[2], and hand kinematics[3]. LFPs can be recorded on hundreds of electrodes simultaneously, resulting in large, complex, and high-dimensional datasets. Successful analysis of LFP data thus requires a technique that can scale with the dataset and produce meaningful predictions based on a limited number of trials. LFPs from the primary motor cortex have been incorporated into a neural critic to classify trial reward expectation as part of an autonomously updating BMI[4].

Convolutional Neural Networks (CNNs) are a computational structure used for classification, commonly of images. CNNs have previously been applied to LFPs for localization of deep brain stimulation probes[5], decoding human behaviors[6], and detection of epileptogenic biomarkers[7, 8]. For somatosensory applications, CNNs have been applied to classify recordings from multicontact cuff electrodes on the sciatic nerve[9]. While used in the periphery, this technique can also be applied in the central nervous system, which is described here. LFP recordings from the rat cortex were converted into spatiotemporal signatures in the form of image files. Pretrained CNN models were fine-tuned on this dataset to create a classifier that could determine a cutaneous stimulus's location from up to 8 different sites on the rat forepaw.

II. Methods

A. Local Field Potential Recordings

LFP data used in this work was collected as part of a study published previously[10]. In short, female Long-Evans rats were implanted with either a 32 channel Utah Array (Blackrock Microsystems) or a 4 shank 32 channel multi-contact array (NeuroNexus). Cutaneous stimuli were performed using an electronically controlled precision tactor system at eight different sites on the rat forepaw. This system was connected to a neural signal acquisition system (Tucker-Davis Technologies) to record stimulus onsets synchronously with the neural data. Data were bandpass filtered with cutoff frequencies at 5Hz and 200Hz, with a sampling rate of 610Hz. Each recording session lasted approximately 30 minutes.

For the analysis in this work, recordings from three rats were used.

FIGURE 1

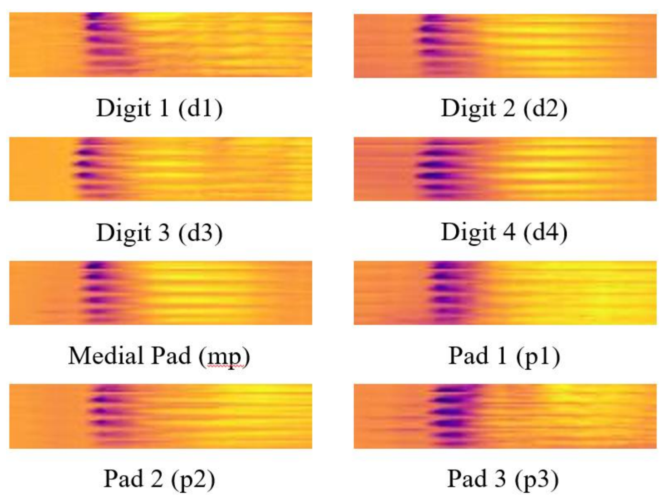

Figure 1. Example Spatiotemporal signatures from each stimulus location on the rat forepaw

B. Creation of Spatiotemporal Signatures

All code in this work was executed in Google Colab using a GPU accelerated runtime. The h5py package was used to import the original MATLAB formatted datasets as HDF5

*Research supported by DARPA REPAIR project N66001-10-C-2008, the New York State Spinal Cord Injury Research Board Awards 73525 (C30600GG) and 73689 (DOH01C30838GG3450000), and NIH grants 1R01NS092894-01 and 1R01NS124222-01

B. A. See, is with the Biomedical Engineering Department at the University of Houston, Houston, TX 77004 USA. (e-mail: basee@uh.edu).

files usable in Python, which was used for all the data processing and network training. A timestamp was associated with a corresponding tactile stimulus location for each trial. Using these timestamps as a starting point, a matrix was created from the underlying dataset, with each row representing a recording channel and each column representing a single time sample. Other hyperparameters being held equal, adjusting the time length of the signatures resulted in variable accuracy of the resulting models. A length of 150 samples was chosen as the point where the model did not improve further with additional time data. Using 200 samples showed no performance improvement, while 100 sample length increased the error rate by 4% in preliminary testing. The matrices were then normalized based on each signature's minimum and maximum values and converted into images. This method of signature generation was repeated separately for each animal. Example signatures from one animal are given in Figure 1. The number of signatures generated for each animal depended on the number of separate stimuli performed: 2310, 2400, and 1200 signatures for animals 1, 2, and 3, respectively.

FIGURE 2

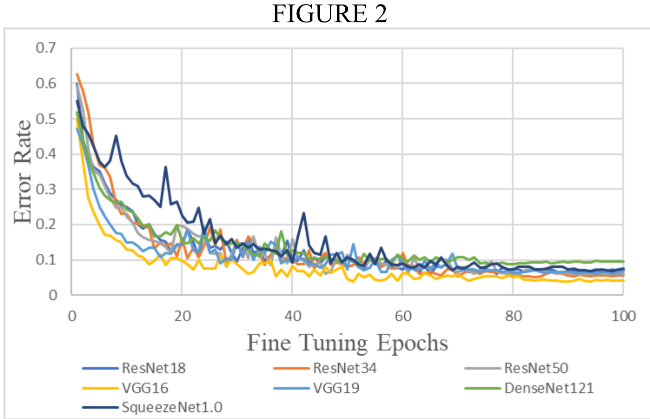

Figure 2. Validation set error rate for different networks at each epoch during training on animal 1

C. *Model Training*

The fastai library was used to train, test, and assess the neural network models created from the LFP data. As the spatiotemporal signatures were created, they were sorted by the location of the stimulus. Additionally, 20% of the data were randomly separated for use as a test set. During data loading for model training, an additional 30% of the dataset was randomly set aside for validation, which provided our primary error_rate metric during training. A Residual Neural Network (ResNet) was fine-tuned on the spatiotemporal signatures and their presorted classes using fastai's fine_tune function. This utilized a transfer learning approach, where a network previously trained on a much larger dataset can be applied to a different dataset. By retraining the output layer of the network, the model retains the excellent feature extraction capabilities of a trained CNN. After multiple iterations, the performance improvement on the validation set saturated by around 100 epochs. Example 100-epoch training sessions are shown in Figure 2. To avoid overfitting the models, 100 epoch fine-tuning was chosen for all models. A dataset with randomized labels was used as a sanity check, which produced a model with an error rate very close to random chance, as expected. The training methodology and subsequent testing were performed separately for each animal.

III. Results

A. *Image Resize Optimization*

Generally, images for training and classification must be the same size and square in shape. All spatiotemporal signatures generated for a given signature sample length are the same size rectangles and underwent the same resizing method for training and prediction. Using the fastai crop resizing method on the images visibly resulted in a loss of information and showed abysmal error rates, so it was discarded as an option. Another available option was padding, where the image is fit into a square along the longer rectangular axis (in this case, the horizontal time sample axis) while padding with zeros outside the rectangular image. While no information is lost using this method, the resulting black bars add a significant amount of empty information that the network must process. Using this method achieved a validation error rate of 8.8%.

Another option tested was squishing the image by stretching it along the shorter axis to fit a square. This method distorts features, albeit consistently across images in the dataset. Using the squish resize method resulted in an error rate of 9.7%.

Example padded and squished images of the spatiotemporal signatures are given in Figure 3. Both showed a significantly lower error rate versus the error rate for random chance for 8 classes of 87.5%. Due to its slightly higher performance, padded images were used for subsequent training.

FIGURE 3

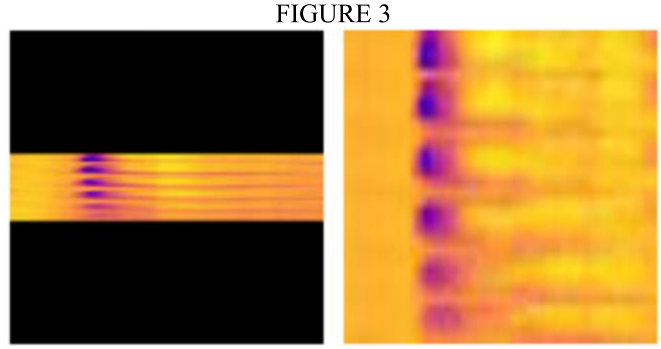

Figure 3. Example padded (left) and squished (right)

B. *Improvements from deeper networks*

The architecture of the neural network used will affect its performance. One key element of the architecture is its depth, the number of layers from the input layer to the output layer. Additional layers can improve the error rate by extracting more complex and general features of an image. This often comes at the cost of decreased model generalization due to a higher degree of overfitting. We tested 3 network depths to assess if further error rate reduction could be achieved. Thus far, all analyses reported used the ResNet18 model, an 18-layer model. Using the same methodology as in previous tests, 34- and 50-layer ResNets were fine-tuned for the classification. ResNet34 achieved an error rate of 7.0%. ResNet50 had an error rate of

4.5% on the validation sets. This improvement of up to 4.3% in error rate demonstrates that deeper networks can be used to enhance the test classification performance with LFPs.

C. *Performance of Multiple CNN Models*

Once hyperparameters and training methodology were optimized, it was necessary to validate the models on the test set, which was set aside before training as a final test of model performance. We also applied this training methodology beyond ResNets to other available pretrained models. Table I compares their error rates on the test sets, which were comparable to validation set performance. At 4.1%, the two VGG models both had the best performance of all the tested models. This suggests that future CNN model training for neural decoding should emphasize these models.

TABLE I

Model	Error Rate
ResNet18	7.4%
ResNet34	5.2%
ResNet50	5.6%
SqueezeNet1.0	6.5%
VGG16	4.1%
VGG19	4.1%
DenseNet121	6.5%
AlexNet	7.8%

D. *Class-Specific Errors and Confusion*

The models in this work predicted 8 classes of different cutaneous stimulus locations. These locations are not equidistant from each other, and therefore classes were expected to show differing levels of similarity between their spatiotemporal signatures. Thus, the degree to which signatures were erroneously classified was expected to vary between classes. Figure 4 shows confusion matrices of ResNet18 predictions for each of the three animals in this work.

As can be seen, the vast majority of classifications are accurate, falling along the diagonal of the matrix where the prediction matches the actual class. There are a small number of random erroneous classifications for each animal. However, some clear systematic issues are observable even for the best performing animal 1 dataset, notably p3 getting confused for d4, mp, or p2.

Animal 2's higher error rate of 8.6% is reflected in its confusion matrix with slightly more inaccurate predictions. Most notably, there are more misclassifications surrounding p1, which is frequently confused with d1, mp, and p2. The results on the first 2 animals could reflect broader receptive fields on the pads versus the digits, which have comparatively low rates of misclassification.

Examining the confusion matrix for animal 3 gives insight into the causes of the much worse 18.8% error rate for this animal's dataset. Notably, there are many random misclassifications between multiple classes rather than mainly concentrated systematic errors.

FIGURE 4

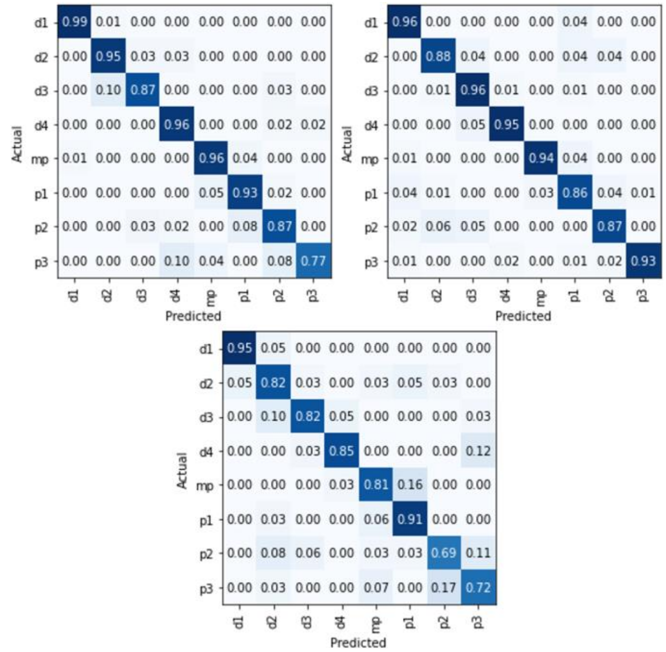

Figure 4. Confusion matrix for animal 1 (top left), animal 2 (top right), and animal 3 (bottom)

IV. Discussion

The error rates achieved by the models trained in this work demonstrate the utility of transfer learning and CNNs for the classification of LFP data from the somatosensory cortex. These results also elucidate the effect the number of training epochs, image resizing methodology, and network depth have on the error rate of the trained models. The fastai library made exploring, testing, and iterating on these models very straightforward. Models could be fully trained in a few minutes, facilitating optimization of the models for prediction, utilizing online GPU processing capabilities. This is in contrast to training CNNs without employing transfer learning, which can take several hours or even longer.

In terms of the final performance demonstrated by the models, CNNs performed comparably to other state of the art learning methods. Notably, a study[11] applying Kernel-based Metric learning to the same 8 class rat forepaw location decoding task reported correct classification rates for 4 different LFP datasets ranging from 85% to 98% for the most accurate models, using Mahalanobis-based metrics that were optimized with either centered alignment or Fisher discriminant analysis. That study also had a wide range of classification accuracy between datasets. While our CNN models only peaked at 96.1% accuracy, this is well within the range of the datasets reported in that study and may also be a result of the variable suitability of the datasets collected for this classification task.

Finally, it is important to address the conceptual and theoretical suitability of using images created from multichannel LFP data as we have here. It would seem that the use of arbitrarily numbered channels on a 2-dimensional array as a dimension alongside time would exceed any reasonable definition of an image. However, while computational activity of the brain is somatotopically mapped, all relevant information transfer may not be entirely local. Thus, relying on strictly spatial ordering in this dimension may not be necessary or even beneficial. Indeed, in the study on classifying spatiotemporal signatures in a peripheral nerve, [9] two different electrode numbering schemes were used to account for the fact that the array had both a radial and longitudinal dimension, similar to our 2D arrays. A similar technique using transfer learning was also used to classify sleep stages using EEG data[12]. The technique has also been applied to non-image data outside the biomedical space, such as mel spectrograms for music genre classification[13]. Furthermore, convolutional neural networks have proven themselves in the field of image classification by extracting features. It is clear to the human eye looking at the examples of LFP spatiotemporal signatures shown in Figure 1 that there are features that distinguish the classes. Therefore, these signatures are not conceptually at odds with the use of a CNN for classification.

V. Conclusion

This work has demonstrated the methodology of fine tuning a convolutional neural network for classifying LFP recordings from the central nervous system based on the location of the applied stimulus. Utilizing this method allows for rapid training of the network and a high level of accuracy that is comparable to other state-of-the-art techniques in the field.

Acknowledgment

The authors thank J. S. Choi for collecting the dataset used in this analysis.

References

[1] Q. Zhang *et al.*, "Local field potential decoding of the onset and intensity of acute pain in rats," *Scientific Reports,* vol. 8, no. 1, p. 8299, 2018/05/29 2018, doi: 10.1038/s41598-018-26527-w.

[2] M. Angjelichinoski, T. Banerjee, J. Choi, B. Pesaran, and V. Tarokh, "Minimax-optimal decoding of movement goals from local field potentials using complex spectral features," *Journal of Neural Engineering,* vol. 16, no. 4, p. 046001, 2019/05/09 2019, doi: 10.1088/1741-2552/ab1a1f.

[3] N. Ahmadi, T. G. Constandinou, and C. Bouganis, "Decoding Hand Kinematics from Local Field Potentials Using Long Short-Term Memory (LSTM) Network," in *2019 9th International IEEE/EMBS Conference on Neural Engineering (NER)*, 20-23 March 2019 2019, pp. 415-419, doi: 10.1109/NER.2019.8717045.

[4] J. An, T. Yadav, M. B. Ahmadi, V. S. A. Tarigoppula, and J. T. Francis, "Near Perfect Neural Critic from Motor Cortical Activity Toward an Autonomously Updating Brain Machine Interface," (in eng), *Annu Int Conf IEEE Eng Med Biol Soc,* vol. 2018, pp. 73-76, Jul 2018, doi: 10.1109/embc.2018.8512274.

[5] M. Hosny, M. Zhu, Y. Su, W. Gao, and Y. Fu, "A novel deep recurrent convolutional neural network for subthalamic nucleus localization using local field potential signals," *Biocybernetics and Biomedical Engineering,* vol. 41, no. 4, pp. 1561-1574, 2021/10/01/ 2021, doi: https://doi.org/10.1016/j.bbe.2021.09.005.

[6] H. M. Golshan, A. O. Hebb, and M. H. Mahoor, "LFP-Net: A deep learning framework to recognize human behavioral activities using brain STN-LFP signals," *Journal of Neuroscience Methods,* vol. 335, p. 108621, 2020/04/01/ 2020, doi: https://doi.org/10.1016/j.jneumeth.2020.108621.

[7] Z. Wang and C. Li, "Classifying cross-frequency coupling pattern in epileptogenic tissues by convolutional neural network[*]," in *2020 42nd Annual International Conference of the IEEE Engineering in Medicine & Biology Society (EMBC)*, 20-24 July 2020 2020, pp. 3440-3443, doi: 10.1109/EMBC44109.2020.9175273.

[8] R. Zuo *et al.*, "Automated Detection of High-Frequency Oscillations in Epilepsy Based on a Convolutional Neural Network," (in English), *Frontiers in Computational Neuroscience,* Original Research vol. 13, 2019-February-12 2019, doi: 10.3389/fncom.2019.00006.

[9] R. G. L. Koh, M. Balas, A. I. Nachman, and J. Zariffa, "Selective peripheral nerve recordings from nerve cuff electrodes using convolutional neural networks," (in eng), *J Neural Eng,* vol. 17, no. 1, p. 016042, Jan 31 2020, doi: 10.1088/1741-2552/ab4ac4.

[10] J. S. Choi, A. J. Brockmeier, D. B. McNiel, L. M. Kraus, J. C. Principe, and J. T. Francis, "Eliciting naturalistic cortical responses with a sensory prosthesis via optimized microstimulation," *J Neural Eng,* vol. 13, no. 5, p. 056007, Oct 2016, doi: 10.1088/1741-2560/13/5/056007.

[11] A. J. Brockmeier, J. S. Choi, E. G. Kriminger, J. T. Francis, and J. C. Principe, "Neural Decoding with Kernel-Based Metric Learning," *Neural Computation,* vol. 26, no. 6, pp. 1080-1107, 2014, doi: 10.1162/NECO_a_00591.

[12] P. Jadhav, G. Rajguru, D. Datta, and S. Mukhopadhyay, "Automatic sleep stage classification using time–frequency images of CWT and transfer learning using convolution neural network," *Biocybernetics and Biomedical Engineering,* vol. 40, no. 1, pp. 494-504, 2020/01/01/ 2020, doi: https://doi.org/10.1016/j.bbe.2020.01.010.

[13] Y. H. Cheng, P. C. Chang, and C. N. Kuo, "Convolutional Neural Networks Approach for Music Genre Classification," in *2020 International Symposium on Computer, Consumer and Control (IS3C)*, 13-16 Nov. 2020 2020, pp. 399-403, doi: 10.1109/IS3C50286.2020.00109.